THE JOURNAL OF BIOLOGICAL CHEMISTRY VOL. 284, NO. 8, pp. 4865–4872, February 20, 2009
© 2009 by The American Society for Biochemistry and Molecular Biology, Inc. Printed in the U.S.A.

Interaction of Tim23 with Tim50 Is Essential for Protein Translocation by the Mitochondrial TIM23 Complex*[S]

Received for publication, September 10, 2008, and in revised form, October 28, 2008 Published, JBC Papers in Press, November 18, 2008, DOI 10.1074/jbc.M807041200

Lada Gevorkyan-Airapetov[‡1], Keren Zohary[‡1], Dušan Popov-Čeleketić[§], Koyeli Mapa[§], Kai Hell[§], Walter Neupert[§], Abdussalam Azem[‡2], and Dejana Mokranjac[§]

From the [‡]Department of Biochemistry, George S. Wise Faculty of Life Sciences, Tel Aviv University, 69778 Tel Aviv, Israel and the [§]Munich Center for Integrated Protein Science, Institute for Physiological Chemistry, University of Munich 81377, Munich, Germany

The TIM23 complex is the major translocase of the mitochondrial inner membrane responsible for the import of essentially all matrix proteins and a number of inner membrane proteins. Tim23 and Tim50, two essential proteins of the complex, expose conserved domains into the intermembrane space that interact with each other. Here, we describe *in vitro* reconstitution of this interaction using recombinantly expressed and purified intermembrane space domains of Tim50 and Tim23. We established two independent methods, chemical cross-linking and surface plasmon resonance, to track their interaction. In addition, we identified mutations in Tim23 that abolish its interaction with Tim50 *in vitro*. These mutations also destabilized the interaction between the two proteins *in vivo*, leading to defective import of preproteins via the TIM23 complex and to cell death at higher temperatures. This is the first study to describe the reconstitution of the Tim50-Tim23 interaction *in vitro* and to identify specific residues of Tim23 that are vital for the interaction with Tim50.

Maintenance and growth of mitochondria depend on the constitutive import of newly synthesized proteins that are encoded by nuclear DNA, translated on cytoplasmic ribosomes as precursors and eventually taken up from the cytosol. The latter process is mediated by several complex sorting and import machineries, protein translocases, and insertases that are located in the outer and inner mitochondrial membranes (1–3). The port of entry for almost all of the precursor proteins is the TOM (translocase of the outer mitochondrial membrane) complex. Once the precursor protein has started to cross the outer membrane through the TOM complex, sorting signals trigger transport to its final destination, a process facilitated by one of the various import complexes (2, 4–6).

The TIM23 (translocase of the inner mitochondrial membrane) complex handles the import of precursor proteins that contain N-terminal targeting signals, which include proteins destined for the matrix as well as some of the inner membrane and intermembrane space (IMS)[3] proteins. The TIM23 complex can be distinguished into two functionally defined parts: a core complex comprised of integral membrane proteins whose subunits are firmly associated with the membrane and the import motor. The core complex comprises three essential proteins: Tim17, Tim23, and Tim50, which make up the receptors and the translocation channel of the complex. Initial translocation of the N-terminal presequence across the inner membrane requires the membrane potential $\Delta\Psi$. Completion of translocation across the inner membrane, however, requires the action of the import motor (2, 7). The import motor consists of an ATP-hydrolyzing chaperone, the 70-kDa mitochondrial heat shock protein (mtHsp70), and Tim44, which recruits the latter to the TIM23 complex (8–10). Other key players in the import motor, the co-chaperone complex Tim14/Pam18–Tim16/Pam16 (11–15), and the nucleotide exchange factor Mge1 (16–18) modulate the activity of mtHsp70 and thereby regulate the binding of the chaperone to the incoming unfolded precursor proteins. Finally, two nonessential membrane proteins, Pam17 and Tim21, modulate the activity of the TIM23 complex in an antagonistic manner. How exactly these proteins exert their function, however, is currently controversial (19, 20).

Tim50 is anchored in the inner membrane with one transmembrane helix and comprises a large C-terminal hydrophilic domain (~350 amino acid residues) that is exposed to the IMS. Presumably this domain is the first component to interact with the precursor protein emerging from the TOM complex and to direct it to the TIM23 import channel (21–23). Tim23 consists of an N-terminal region of ~100 amino acid residues that is hydrophilic and exposed to the IMS and of a C-terminal hydrophobic domain that spans the inner membrane with four transmembrane helices comprising ~120 residues (2, 4, 6). The first ~20 residues of Tim23 are found on the mitochondrial surface (20, 22, 28). Tim23 and Tim50 were proposed to interact via their soluble IMS domains (21, 22). Using *in vivo* chemical cross-linking, two regions on Tim23 were recently identified that mediate interaction with Tim50. The first one lies in the N-terminal domain, and the second one lies in the first transmembrane helix (24).

* This work was supported by German-Israeli Foundation for Scientific Research and Development Grant 753/181 and German-Israeli Project Cooperation Grant F5.1. The costs of publication of this article were defrayed in part by the payment of page charges. This article must therefore be hereby marked "*advertisement*" in accordance with 18 U.S.C. Section 1734 solely to indicate this fact.

[S] The on-line version of this article (available at http://www.jbc.org) contains supplemental Figs. S1–S4.

[1] These authors contributed equally to this work.

[2] To whom correspondence should be addressed. Tel.: 972-3-640-9007; E-mail: azema@tauex.tau.ac.il.

[3] The abbreviations used are: IMS, intermembrane space; DSS, disuccinimidyl suberate; TEV, tobacco etch virus; mtHsp70, 70-kDa mitochondrial heat shock protein; PK, proteinase K; CBB, Coomassie Brilliant Blue.

This is an Open Access article under the CC BY license.

We set out to reconstitute the interaction between Tim23 and Tim50 *in vitro*. We prepared recombinant purified intermembrane space domains of two proteins and studied their interaction by cross-linking and surface plasmon resonance measurements. Also, we identified mutations in Tim23 that abolished its interaction with Tim50. Mitochondria harboring Tim23 with these mutations were deprived in their ability to import precursor proteins via the TIM23 complex. This is the first study to reconstitute the Tim23-Tim50 interaction *in vitro* from recombinant proteins and to identify specific residues on Tim23 that are essential for it.

EXPERIMENTAL PROCEDURES

Materials—Proteinase K (P-6556), V_8 proteinase (P-2922), and DNase (D-5025) were purchased from Sigma. Disuccinimidyl suberate (DSS; 21555) was from Pierce, and complete EDTA-free protease inhibitor mixture (13625900) was from Roche Applied Science.

Construction of NusA-Tim23$_{IMS}$ and NusA-Tim50$_{IMS}$—The sequences encoding the soluble domains of yeast Tim23 (amino acids 1-96) and Tim50 (amino acids 133-476) were amplified by PCR, with a *Saccharomyces cerevisiae* genomic DNA as a template and the primers listed in Table 1. The PCR products were cloned into a modified pET-43.1a(+) vector containing octahistidine-tagged NusA protein (25) (kindly provided by Dr. Joel Hirsch) and a cleavage site for the TEV protease. The construct was engineered in such a way that the histidine tag and NusA were removed upon TEV protease treatment. The *Escherichia coli* strain BL21(DE3) was used as a host for the expression of NusA-Tim23$_{IMS}$ or NusA-Tim50$_{IMS}$ fusion proteins.

Purification of Tim23$_{IMS}$ and Tim50$_{IMS}$—Bacteria were grown for ~3 h at 37 °C in 6 L of LB medium containing 100 μg/ml ampicillin. Upon reaching an A_{600} of 0.6, the temperature was lowered to 16 °C, and protein expression was induced with 1 mM isopropyl β-D-1-thiogalactopyranoside overnight. Bacteria were collected by centrifugation at 5,000 rpm for 10 min and homogenized in 60 ml of lysis buffer containing 50 mM Tris-HCl, pH 7.4, 200 mM NaCl, 1% Triton X-100, 20 mM imidazole, 0.05 mg/ml lysozyme, 45 mg/ml DNase, 2 mM phenylmethylsulfonyl fluoride, and one tablet of complete EDTA-free protease inhibitor mixture. After incubation for 15 min on ice, the bacteria were disrupted using a microfluidizer. Insoluble material was removed by centrifugation at 14,000 rpm for 30 min at 4 °C. The soluble fraction was loaded onto a nickel-nitrilotriacetic acid-agarose column (20 ml) pre-equilibrated with buffer A (50 mM Tris-HCl, pH 7.4, 200 mM NaCl, 20 mM imidazole). The column was washed with three volumes of buffer A until a stable base line was reached. The fractions were eluted with a linear gradient (0–50%, 90 ml) of buffer B (buffer A containing 1 M imidazole). The fractions enriched with the protein were pooled and treated with TEV protease (TEV:protein, 1:40 w/w) overnight at 4 °C in a dialysis bag against 5 liters of buffer A. The protein was then passed over a second nickel-nitrilotriacetic acid-agarose column to remove in one step the TEV protease, which contained an uncleavable octahistidine tag, NusA, which remained after digestion of the fusion protein and also contained the histidine tag, along with the nondigested material and nonspecifically bound proteins. Fractions enriched with the desired protein were concentrated and loaded onto a HiLoad 16/60 Superdex 200 column (total bead volume, 90 ml; Amersham Biosciences) pre-equilibrated with 20 mM NaHEPES, pH 7.4, 200 mM NaCl, and 5% glycerol at a flow rate of 1 ml/min. Fractions with the desired protein were concentrated using Vivaspin protein concentrators (Vivascience; molecular weight cut-off of 5,000 for Tim23$_{IMS}$ and 10,000 for Tim50$_{IMS}$), divided into aliquots, and flash-frozen in liquid N_2. All of the purification procedures were carried out at 4 °C.

Mutagenesis—Site-directed mutants were created according to the protocol of Stratagene, using the primers listed in Table 1.

Circular Dichroism—All of the CD measurements were carried out with an Aviv CD spectrometer model 202 over the range of 260-190 nm at a scan rate of 1 nm/s, using a cell with a path length of 0.1 mm. Each spectrum is an average of five scans. The raw data were corrected by subtracting the contribution of the buffer to the CD signal. The data were smoothed and converted to molar ellipticity units. The measurements were taken at a constant temperature of 25 °C in buffer containing 20 mM NaHEPES, pH 7.4, 200 mM NaCl, and 5% glycerol, with a protein concentration of 1 mg/ml.

Thermal Aggregation Assay for Tim23$_{IMS}$ and Tim50$_{IMS}$—Aliquots (0.4 mg/ml) of Tim23$_{IMS}$ or Tim50$_{IMS}$ in 20 mM NaHEPES, pH 7.4, 200 mM NaCl, 5% glycerol were incubated at different temperatures for 15 min and then centrifuged at 14,000 rpm for 5 min at room temperature to obtain aggregated (pellet) and soluble (supernatant) fractions. The proteins in each fraction were analyzed by SDS-PAGE and staining with Coomassie Brilliant Blue (CBB).

Limited Proteolysis of Tim23$_{IMS}$ and Tim50$_{IMS}$—V_8 Protease (0.01 mg/ml) was used to digest 0.2 mg/ml Tim23$_{IMS}$ or Tim50$_{IMS}$. PK (0.2 μg/ml) was added to 0.4 mg/ml protein. The reactions were allowed to proceed on ice in 20 mM NaHEPES, pH 7.4, and 200 mM NaCl. Time-dependent proteolysis of proteins was followed by SDS-PAGE and CBB staining.

Cross-linking Experiments—Cross-linking reactions were carried out with 1 mM DSS at room temperature for 1 h in 20 mM NaHEPES, pH 7.4, 200 mM NaCl, 5 mM $MgCl_2$, 50 mM KCl, and 5% glycerol at a protein concentration of 10 μM. The reaction was stopped by the addition of SDS-containing sample buffer. The cross-linked products were separated by SDS-PAGE using a gradient of 8–16% acrylamide and stained with CBB.

Surface Plasmon Resonance—The experiments were performed with a ProteOn XPR36 instrument (Bio-Rad). This system uses an SPR-based detector to monitor formation of complexes between analytes and ligand molecules. The sensor chip (GLC) was activated for 80 s with a mixture of 0.1 M EDC and 0.025 M sulfo-NHS (TS-Pierce). Immediately after activation, 20 μg of Tim23$_{IMS}$ (wild type or mutant) in 1 volume of buffer C (20 mM NaHEPES, pH 7.4, 200 mM NaCl, 5% glycerol, 0.001% Tween) were diluted with 4 volumes of buffer D (10 mM sodium acetate, pH 3.5) and injected across channel/s (400 s at a flow rate of 30 μl/min). One channel, which was treated with the buffer without protein, served as a reference. Finally, the channels were blocked with 1 M ethanolamine-HCl, pH 8.5, for 200 s. Tim23$_{IMS}$ was coupled at response levels of ~800 RU in a chan-

nel. The chip was rotated at 90°, the channels were washed for 30 min with buffer C, and six different concentrations of $Tim50_{IMS}$ were simultaneously injected at a flow rate of 30 μl/min for an association phase of 200 s, which was followed by a 600-s dissociation phase.

Yeast Strains and Media—Wild type yeast strain YPH499 was used (26). To generate the strain containing a chromosomal deletion of TIM23 rescued with Tim23 on URA plasmid, YPH499 cells were transformed with pVT-U plasmid (27) carrying the wild type copy of Tim23 under the control of the ADH promoter. The chromosomal copy of TIM23 was subsequently deleted by the KAN cassette using homologous recombination. This strain was designated Δ23 + 23URA. To generate yeast strains carrying mutant versions of Tim23 instead of wild type, Tim23 mutants were cloned into centromeric plasmid pRS315 (26) under control of the endogenous promoter and 3′-untranslated region and transformed into Δ23 + 23URA. An empty pRS315 and the plasmid carrying the wild type copy of Tim23 were transformed as controls. Yeast cells that had lost the URA plasmid were selected on medium containing 5-fluoroorotic acid.

Yeast cells were normally grown on lactate medium containing 0.1% (w/v) glucose at 30 °C. To exclude possible secondary effects, for import assays yeast cells were grown at 24 °C. For drop dilution assays, 10-fold serial dilutions of yeast cells were spotted on YPG plates and incubated at 24, 30, and 37 °C for 2 days.

Miscellaneous—Coimmunoprecipitation experiments were performed according to published procedures (11). Import into isolated mitochondria was done as described previously (11) with the modification that mitochondria were preincubated for 10 min at 37 °C before the addition of radiolabeled precursor proteins.

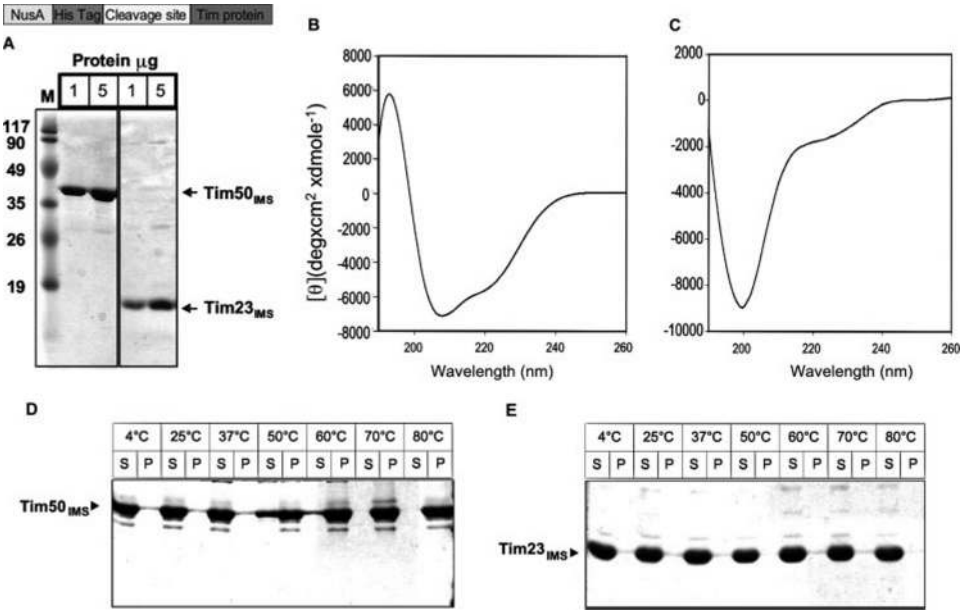

FIGURE 1. **Folding and stability of isolated IMS domains of Tim50 ($Tim50_{IMS}$) and Tim23 ($Tim23_{IMS}$).** *A*, SDS-PAGE of purified $Tim50_{IMS}$ and $Tim23_{IMS}$ (each 1 and 5 μg). Staining with Coomassie Brilliant Blue. *B* and *C*, CD spectra at 25 °C of $Tim50_{IMS}$ and $Tim23_{IMS}$, respectively. *D* and *E*, thermal stability of $Tim50_{IMS}$ (*D*) and $Tim23_{IMS}$ (*E*) samples were incubated at the indicated temperatures for 15 min, separated into a soluble fraction (*S*) and aggregate in the pellet (*P*) by centrifugation, and analyzed by SDS-PAGE and CBB staining.

RESULTS

Properties of Purified $Tim23_{IMS}$ and $Tim50_{IMS}$—We purified the soluble intermembrane space domains of Tim23 and Tim50 after expression in *E. coli*. (Fig. 1*A*). Their secondary structure was determined by CD spectroscopy. The spectrum of $Tim50_{IMS}$ showed that it was folded with a high content of α-helices and β-sheets (Fig. 1*B*). $Tim23_{IMS}$ yielded a spectrum indicative of an unstructured protein; however, there were also indications of the presence of some structured elements (Fig. 1*C*). Protease digestion experiments (supplemental Fig. S1) confirmed that $Tim50_{IMS}$ is a tightly folded protein, whereas $Tim23_{IMS}$ is largely

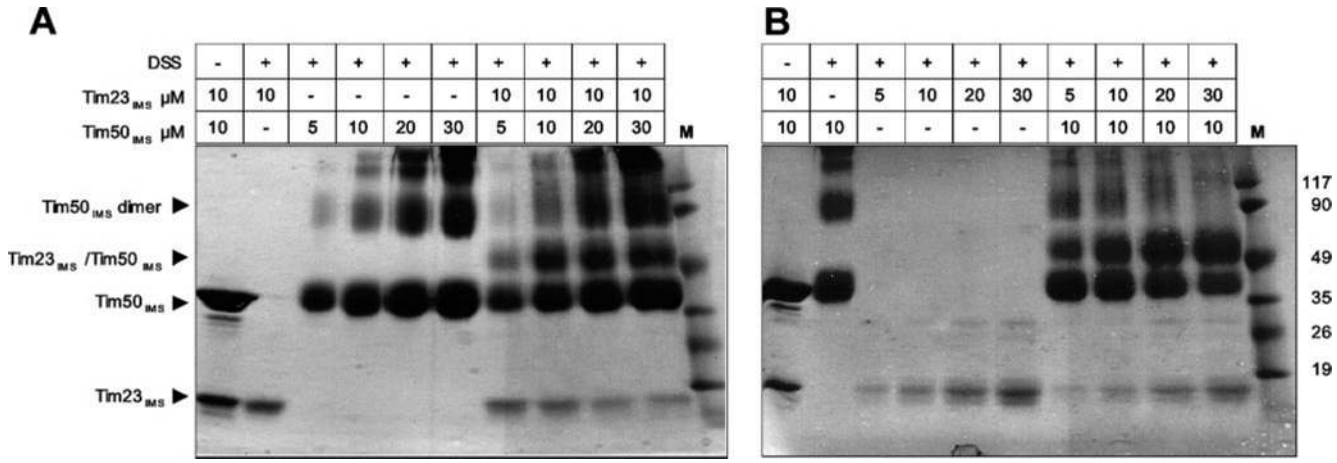

FIGURE 2. **Complex formation of the isolated intermembrane space domains of Tim50 and Tim23 detected by chemical cross-linking.** *A*, purified $Tim23_{IMS}$ (10 μM) was incubated for 10 min with increasing concentrations of purified $Tim50_{IMS}$ and then for 1 h with 1 mM DSS at 25 °C. *B*, purified $Tim50_{IMS}$ (10 μM) was incubated with increasing amounts of $Tim23_{IMS}$ and treated as in *A*. Cross-linked products were analyzed by SDS-PAGE and staining with CBB.

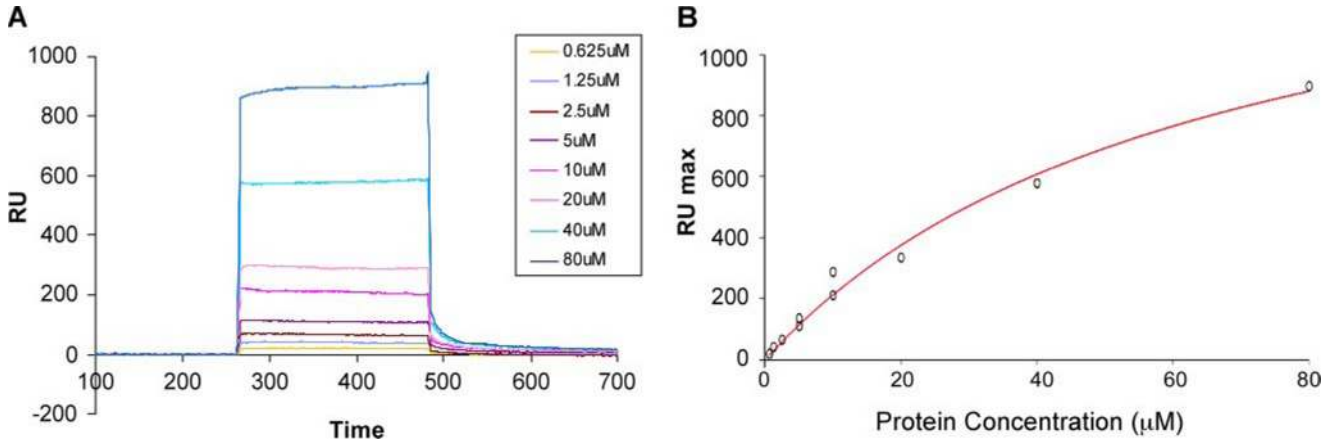

FIGURE 3. **Complex formation of the isolated intermembrane space domains of Tim50 and Tim23 measured by surface plasmon resonance.** *A*, $Tim23_{IMS}$ was immobilized at a density of ~800 RU in the channel. The chip was rotated at 90°, and six different concentrations of $Tim50_{IMS}$ analyte were injected simultaneously at a flow rate of 30 μl/min for a 200-s association phase, followed by a 600-s dissociation phase. *B*, K_D of the interaction, calculated by Bia-Evaluation (BIACORE).

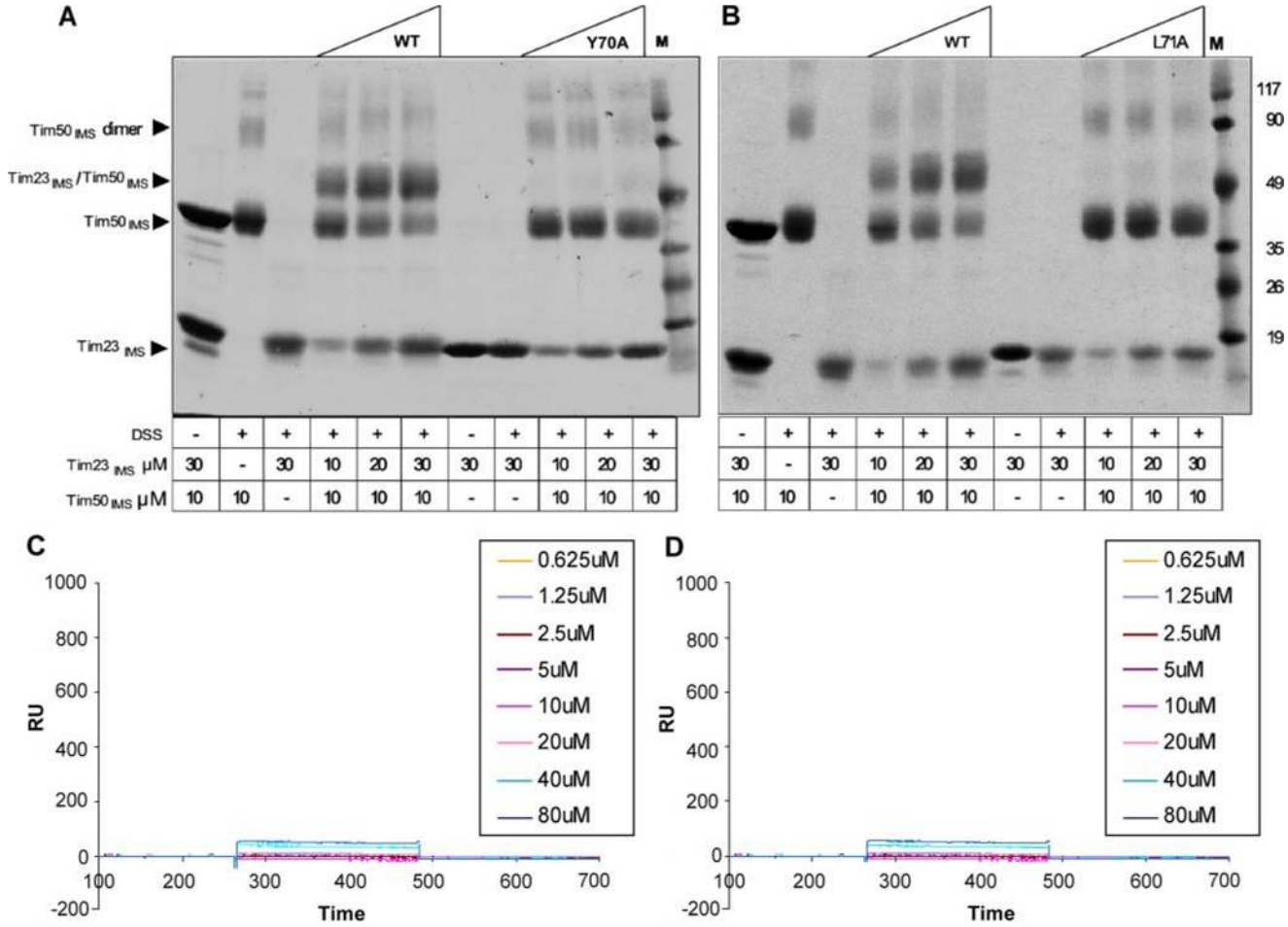

FIGURE 4. **Interaction of $Tim23_{IMS}$ mutants with $Tim50_{IMS}$ determined by cross-linking and surface plasmon resonance.** *A* and *B*, mutants Y70A and L71A, respectively, of $Tim23_{IMS}$ were subjected to chemical cross-linking, as described for Fig. 2. *C* and *D*, surface plasmon resonance analysis of interaction of mutants Y70A and L71A, respectively, of $Tim23_{IMS}$ with $Tim50_{IMS}$. The experimental conditions were as in Fig. 3. *WT*, wild type.

unstructured. Interestingly, programs that predict secondary structures on the basis of primary sequences suggest ~85% of the IMS domain of Tim23 to be unstructured (supplemental Fig. S2).

Next we examined the stability of the purified IMS domains. The thermal stability of both proteins was assessed by following their denaturation. Aggregation of $Tim50_{IMS}$ started at 50 °C and was complete at 60 °C (Fig. 1*D*). Thermal denaturation was also followed by recording the CD spectrum at 222 nm. A T_m value of 52.5 °C was measured (supplemental Fig. S3). Interestingly, $Tim23_{IMS}$ did not aggregate but remained completely soluble at all temperatures examined (up to 80 °C) (Fig. 1*E*). The

TABLE 1
Primers used in this study

$Tim50_{IMS}$	GGATCCATGAGGGATTGGGAGCCTCAAG
	GAATTCTTATTTGGATTCAGCAATCTTC
$Tim23_{IMS}$ (wild type)	GGATCCATGTCGTGGCTTTTTGGAG
	GAATTCCAGTCATCGGTCCACCCACGG
$Tim23_{IMS}$ (P60A)	ACCGCTAGGCTGCATGCGTTGGCTGGTCTAGAC
	GTCTAGACCAGCCAACGCATGCAGCCTAGCGGT
$Tim23_{IMS}$ (D65A)	CATCCTTTGGCTGGTCTAGCAAAGGGTGTGGAGTATTTAG
	CTAAATACTCCACACCCTTTGCTAGACCAGCCAAAGGATG
$Tim23_{IMS}$ (K66A)	CTTTGGCTGGTCTAGACGCAGGTGTGGAGTATTTAG
	CTAAATACTCCACACCTGCGTCTAGACCAGCCAAAG
$Tim23_{IMS}$ (Y70A)	GACAAGGGTGTGGAGGCTTTAGATCTGGAAG
	CTTCCAGATCTAAAGCCTCCACACCCTTGTC
$Tim23_{IMS}$ (L71A)	CAAGGGTGTGGAGTATGCAGATCTGGAAGAAGAAC
	GTTCTTCTTCCAGATCTGCATACTCCACACCCTTG
$Tim23_{IMS}$ (G83A)	CCTCGTTAGAAGCCTCACAGGGTCTG
	CAACCCTGTGAGGCTTCTAACGAGG
$Tim23_{IMS}$ (R91A)	GGTCTGATCCCTTCCGCTGGGTGGACCGATGACC
	GGTCATCGGTCCACCCAGCGGAAGGGATCAGACC
$Tim23_{IMS}$ (D95A)	CCTTCCCGTGGGTGGACCGCTGACCTATGTTACGG
	CCGTAACATAGGTCAGCGGTCCACCCACGGGAAGG
$Tim23_{IMS}$ (Y70L71AA)	GTCTAGACAAGGGTGTGGAGGCAGCAGATCTGGAAGAAGAACAAC
	GTTGTTCTTCTTCCAGATCTGCTGCCTCCACACCCTTGTCTAGAC

TABLE 2
Dissociation constants obtained using SPR

Tim23 strain	K_D
Wild type	57.9
P60A	156
Y70A	ND[a]
L71A	ND
G83A	30.6

[a] ND, no binding detected.

CD spectrum of $Tim23_{IMS}$ remained unchanged even at temperatures as high as 80 °C (not shown). In summary, the isolated $Tim50_{IMS}$ protein was folded with a well defined secondary structure. In contrast, $Tim23_{IMS}$ appeared to be essentially unstructured.

Reconstitution of Tim23-Tim50 Interaction Using Purified $Tim23_{IMS}$ and $Tim50_{IMS}$—To detect an interaction between the isolated $Tim23_{IMS}$ and $Tim50_{IMS}$ domains, we used two methods. First, they were incubated, separately or together, with the cross-linking agent DSS. The cross-linked adducts were then analyzed by SDS-PAGE. With $Tim23_{IMS}$ no cross-linked species were observed (Fig. 2). In contrast, $Tim50_{IMS}$, after exposure to DSS, yielded a pattern comprising not only monomers but also dimers and higher oligomers (Fig. 2). Incubation of $Tim23_{IMS}$ in the presence of DSS and increasing concentrations of $Tim50_{IMS}$ led to the formation of a cross-linked product, which corresponded in size to an adduct of the two proteins. This was confirmed by Western blotting using antibodies raised against both proteins (not shown). The same result was obtained when the concentration of $Tim50_{IMS}$ was kept constant (10 μM), and the concentration of $Tim23_{IMS}$ was increased (Fig. 2*B*).

Concentration-dependent complex formation between $Tim23_{IMS}$ and $Tim50_{IMS}$ was also observed using surface plasmon resonance (Fig. 3*A*). Dissociation of the complex occurred upon washing with buffer. The K_D of the interaction of $Tim23_{IMS}$ and $Tim50_{IMS}$, calculated from the maximal SPR signal as a function of the concentrations, was 60 μM (Fig. 3*B*). In summary, interaction of the purified IMS domains of Tim23 and Tim50 can be demonstrated *in vitro* using both chemical cross-linking and SPR.

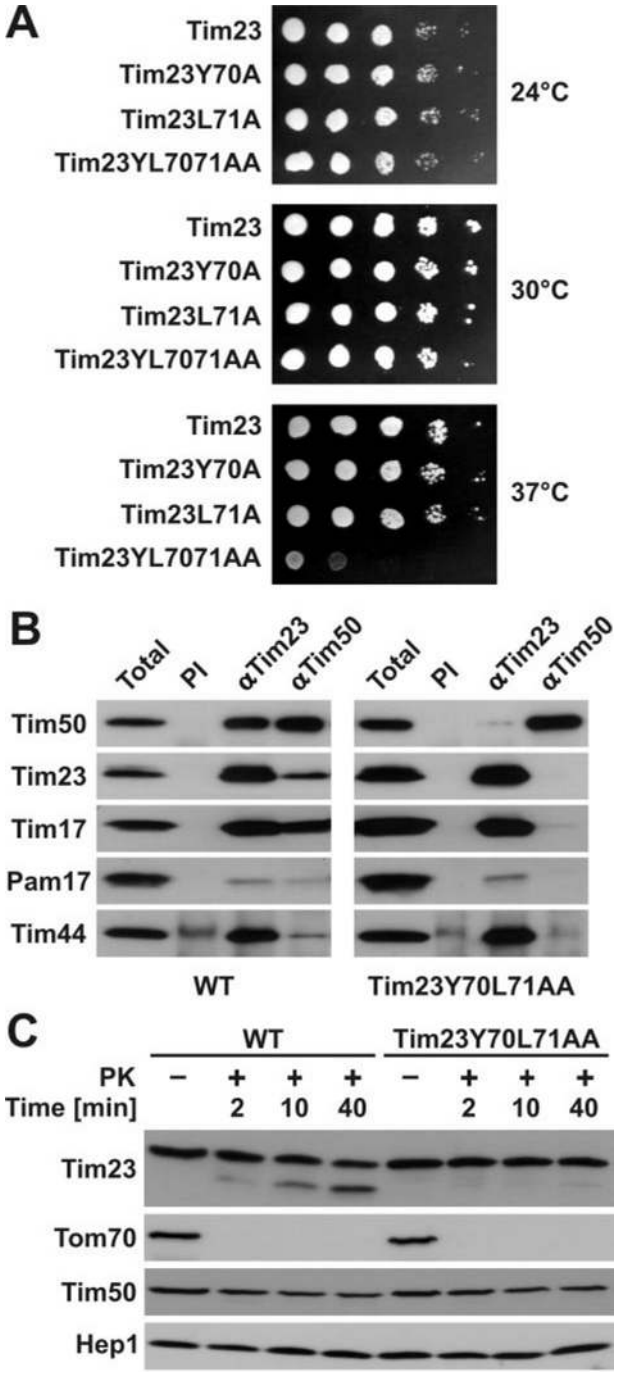

FIGURE 5. **Phenotypes of mutations in the intermembrane space domain of Tim23.** *A*, 10-fold serial dilutions of yeast cells carrying wild type (*WT*) Tim23 or Y70A, L71A, or Y70L71AA mutants were spotted onto YPG plates and grown at the indicated temperatures for 2 days. *B*, mitochondria isolated from wild type or cells carrying the Y70AL71A double mutation in Tim23 were solubilized with digitonin and subjected to immunoprecipitation using affinity purified antibodies to Tim23 and Tim50. Antibodies from preimmune serum were used as a control. Total and immunoprecipitated fractions were analyzed by SDS-PAGE followed by immunodecoration with indicated antibodies. *C*, mitochondria as above were incubated in the presence or absence of PK for the indicated times and subsequently analyzed by SDS-PAGE followed by immunodecoration with the depicted antibodies. Tom70, Tim50, and Hep1 were used as marker proteins for the outer membrane, intermembrane space, and the matrix, respectively.

Identification of Tim23 Mutants Whose Interaction with Tim50 Is Impaired—To identify amino acid residues that participate in complex formation of Tim50 and Tim23, we

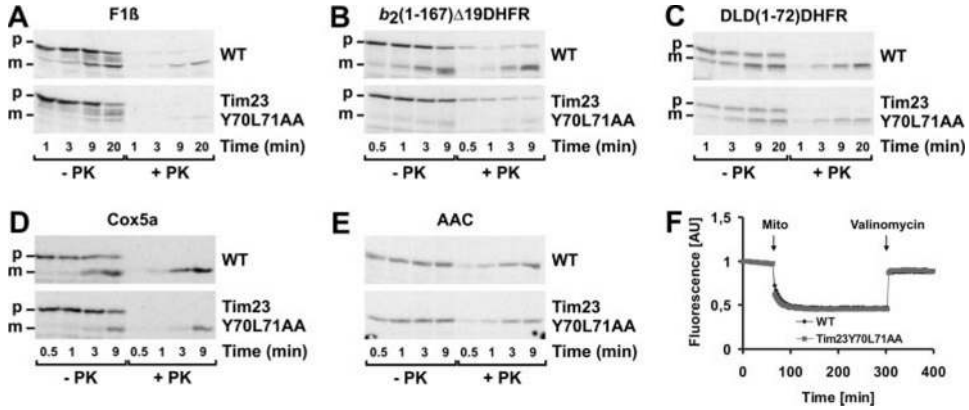

FIGURE 6. **Import of precursor proteins into isolated mitochondria from wild type and Tim23Y70A,L71A mutant cells.** Various mitochondrial preproteins (*A–E*) were synthesized *in vitro* in the presence of [^{35}S]methionine and incubated with isolated mitochondria. At the indicated time points the aliquots were removed and diluted into ice-cold buffer containing valinomycin to stop further import. One half of each sample was treated with proteinase K to digest nonimported material. The samples were subsequently analyzed by SDS-PAGE and autoradiography. *A*, F1β, precursor of the β-subunit of the F1 part of F_0F_1-ATPase. *B*, b_2(1–167)Δ19DHFR, precursor protein consisting of the first 167 residues of yeast cytochrome b_2 with the deleted sorting signal fused to full-length dihydrofolate reductase from mouse. *C*, DLD(1–72)DHFR, precursor protein consisting of the first 72 residues of the yeast D-lactate dehydrogenase fused to the full-length mouse DHFR. *D*, precursor of subunit 5a of the cytochrome *c* oxidase complex from yeast. *E*, *AAC*, precursor of the ATP/ADP carrier. *F*, membrane potential of wild type (*WT*) and mutant mitochondria was assessed by fluorescence quenching with $DiSC_3(5)$.

mutated eight amino acids of $Tim23_{IMS}$, which, in view of their high evolutionary conservation, were suspected to be of functional importance (supplemental Fig. S4). The $TIM23_{IMS}$ domains of these mutants were prepared as described above for wild type. Upon chemical cross-linking only two mutants (Y70A and L71A) showed impaired interaction with $Tim50_{IMS}$ as compared with wild type (Fig. 4, *A* and *B*, and data not shown). Analysis by SPR demonstrated virtually complete lack of interaction of $Tim23_{IMS}$Y70A and $Tim23_{IMS}$L71A with $Tim50_{IMS}$ (Fig. 4, *C* and *D*). The mutant P60A showed a reduction of its K_D relative by a factor of three as compared with wild type (Table 2).

Examination of Tim23 Mutants in Vivo—In view of the striking loss of interaction displayed by the Y70A and L71A mutants, we analyzed them further with regard to their effects in intact yeast cells. We introduced plasmids carrying Tim23Y70A, Tim23L71A, or the double mutation into a yeast strain containing a chromosomal deletion of TIM23, which could be rescued by the wild type copy of Tim23 on the URA plasmid. After shuffling the URA plasmids out on medium containing 5-fluoro-orotic acid, yeast strains harboring only the mutant forms of Tim23 were obtained. Whereas the single mutants displayed no obvious growth defect under the conditions analyzed, the Tim23Y70A,L71A double mutant showed temperature-sensitive growth and was inviable at 37 °C (Fig. 5*A*). We therefore chose to further investigate only the double mutant. In mitochondria isolated from this strain grown at permissive temperature, the stability of Tim23 was unaffected, and the endogenous levels were observed to be unchanged (data not shown). The interaction between Tim23 and Tim50 in wild type and mutant mitochondria was analyzed by coimmunoprecipitation. The complex between Tim23 and Tim50 observed in wild type was not detected in the Tim23 double mutant (Fig. 5*B*). The same result was obtained irrespective of whether antibodies to Tim23 or to Tim50 were used for immunoprecipitation. Interestingly, the interaction of Tim23 with other subunits of the TIM23 complex such as Tim17, Tim44, and Pam17 was not affected by these mutations. This demonstrates the specific involvement of the respective residues in the interaction of the IMS domain of Tim23 with Tim50.

The first ~20 residues of Tim23, normally accessible to the externally added protease in intact mitochondria, were found in a protease-protected location in mitochondria lacking Tim50 (22). We tested whether the presence of Tim50 *per se* is required for the exposure of Tim23 on the mitochondrial surface, or whether this process depends on the interaction of two proteins. In mitochondria having Tim23 double mutant, no clipping of Tim23 was observed even after prolonged exposure to PK (Fig. 5*C*). In contrast, in wild type mitochondria Tim23 was cleaved by externally added PK in a time-dependent manner. Taken together, these results demonstrate that the mutations that abolish the formation of the Tim23-Tim50 complex *in vitro* also affect their interaction *in organelle* and that this interaction is essential for viability of yeast cells and for exposure of Tim23 on the mitochondrial surface.

Finally, we analyzed the import of proteins into mitochondria isolated from cells carrying the Tim23Y70A,L71A mutation. Precursor proteins whose import is dependent on the TIM23 complex were imported into mitochondria with strongly reduced efficiency as compared with the wild type (Fig. 6). This was observed both for proteins targeted to the matrix, exemplified here by F1β and b2ΔDHFR, and to the inner membrane, exemplified by DLD(1–72)DHFR and Cox5a. In contrast, the import of proteins independent of the TIM23 complex, such as ATP/ADP carrier, was virtually unimpeded in mutant mitochondria. Also, mutant mitochondria had essentially the same membrane potential as the wild type, excluding secondary effects on import (Fig. 6*F*). In summary, these results demonstrate that the interaction between Tim23 and Tim50 is essential for efficient import by the TIM23 complex in both its translocation and insertion modes.

DISCUSSION

Tim23 is the central component of the TIM23 complex in which it performs a number of functions. Its C-terminal part is integrated in the inner membrane and is involved in the formation of the translocation channel that mediates the passage of unfolded precursor proteins through the inner membrane (1–3). The N-terminal hydrophilic region of yeast Tim23 is located in the intermembrane space and appears to have two functionally distinct segments. The first ~20 amino acid residues can span the outer membrane in a dynamic fashion,

actively responding to the translocation state of the complex (20, 28). The second part of the N-terminal domain serves several purposes. Early work demonstrated that it is involved in the membrane potential-dependent dimerization of Tim23 and in substrate recognition (29). More recent work showed that it interacts with the intermembrane space domain of Tim50 (21, 22, 30).

In the present study we established two independent assays to reconstitute the interaction between the intermembrane space domains of Tim23 and Tim50 *in vitro* using recombinant proteins. In addition, we identified residues that are essential for this interaction. The mutations of conserved residues Y70A and L71A on Tim23 abolished its interaction with Tim50 *in vitro*. Interestingly, these two residues map to the same region of Tim23 that was recently found by cross-linking to be in close proximity to Tim50 (24).

The results we obtained in *in vitro* experiments are in complete agreement with those obtained *in vivo*. Yeast cells carrying the double Y70A and L71A mutations in Tim23 were not able to grow at 37 °C, and the interaction between Tim23 and Tim50 was destabilized even at permissive temperatures. Intriguingly, destabilization of Tim23-Tim50 interaction did not lead to destabilization of Tim23 interaction with other components of the TIM23 complex, such as Tim17 and Tim44. This result supports the notion that the interaction between Tim50 and Tim23 is rather independent of the rest of the translocase (21–23).

The interaction between the intermembrane space domains of Tim23 and Tim50 is crucial for the function of the TIM23 complex. Mitochondria isolated from cells containing a mutant form of Tim23 imported TIM23 substrates with reduced efficiency as compared with wild type. Interestingly, both laterally sorted substrates and those completely translocated into the matrix were affected in their import. This demonstrates that Tim23 cooperates with Tim50 in both the translocation and insertion modes of the translocase.

The intermembrane space domains of Tim23 and Tim50 apparently form a minimal binding interface required for the interaction of these two proteins. However, it is questionable whether Tim23 and Tim50 interact solely through their soluble domains because we observed a relatively low K_D for the interaction. Indeed, recent work suggested additional interaction surfaces involving the first transmembrane domain of Tim23 (24). In addition, the transmembrane domain of Tim50 appears to have a stabilizing role in the Tim23-Tim50 interaction.[4]

It is intriguing that the isolated intermembrane space domains of Tim23 and Tim50 interact with each other despite the fact that Tim23 is largely unfolded as shown by its CD spectrum. This could well reflect the actual folding state of this domain *in vivo* because its very N-terminal segment has the apparent ability to insert into and deinsert from the outer membrane in a precursor- and Tim50-dependent manner (Refs. 20 and 22 and this work) underlying the apparent necessity for a high conformational flexibility. Also, this domain was found to be extremely protease-sensitive in mitochondria with compromised outer membrane (28). Programs for the prediction of secondary structure failed to suggest major structural elements in the N-terminal domain of Tim23 (supplemental Fig. S2). Interestingly, the two amino acid residues we identified as contributing to the interaction of Tim23 with Tim50 are found in a region that is predicted to be folded into a short β-strand. Natively unstructured (or unfolded) regions were recognized as important mediators of interactions between partner proteins and suggested to undergo folding upon binding to their targets (31). It is therefore tempting to speculate that the substantial unstructured region of $Tim23_{IMS}$ folds into a native conformation upon its association with one of the other components of the mitochondrial protein import machinery or with substrate proteins. We propose that a conformational flexibility of Tim23 is required for its insertion into/deinsertion from the outer mitochondrial membrane, binding and transfer of precursor proteins through the translocation channel into the matrix, and triggering lateral opening of the channel in the case of precursors that are inserted into the inner membrane.

Acknowledgments—We thank Prof. Gideon Schreiber for valuable advice with the SPR experiments, Dr. Yanay Ofran for help on analysis of secondary structures, and Petra Robisch and Marica Malesic for expert technical assistance.

REFERENCES

1. Schatz, G., and Dobberstein, B. (1996) *Science* **271,** 1519–1526
2. Neupert, W., and Herrmann, J. M. (2007) *Annu. Rev. Biochem.* **76,** 723–749
3. Bolender, N., Sickmann, A., Wagner, R., Meisinger, C., and Pfanner, N. (2008) *EMBO Rep.* **9,** 42–49
4. Pfanner, N. (2000) *Curr. Biol.* **10,** R412–R415
5. Rapaport, D. (2005) *J. Cell Biol.* **171,** 419–423
6. Koehler, C. M. (2004) *Annu. Rev. Cell Dev. Biol.* **20,** 309–335
7. Voos, W., and Rottgers, K. (2002) *Biochim. Biophys. Acta* **1592,** 51–62
8. Kronidou, N. G., Oppliger, W., Bolliger, L., Hannavy, K., Glick, B. S., Schatz, G., and Horst, M. (1994) *Proc. Natl. Acad. Sci. U. S. A.* **91,** 12818–12822
9. Rassow, J., Maarse, A. C., Krainer, E., Kubrich, M., Muller, H., Meijer, M., Craig, E. A., and Pfanner, N. (1994) *J. Cell Biol.* **127,** 1547–1556
10. Schneider, H. C., Berthold, J., Bauer, M. F., Dietmeier, K., Guiard, B., Brunner, M., and Neupert, W. (1994) *Nature* **371,** 768–774
11. Mokranjac, D., Sichting, M., Neupert, W., and Hell, K. (2003) *EMBO J.* **22,** 4945–4956
12. Kozany, C., Mokranjac, D., Sichting, M., Neupert, W., and Hell, K. (2004) *Nat. Struct. Mol. Biol.* **11,** 234–241
13. D'Silva, P. D., Schilke, B., Walter, W., Andrew, A., and Craig, E. A. (2003) *Proc. Natl. Acad. Sci. U. S. A.* **100,** 13839–13844
14. Truscott, K. N., Voos, W., Frazier, A. E., Lind, M., Li, Y., Geissler, A., Dudek, J., Muller, H., Sickmann, A., Meyer, H. E., Meisinger, C., Guiard, B., Rehling, P., and Pfanner, N. (2003) *J. Cell Biol.* **163,** 707–713
15. Frazier, A. E., Dudek, J., Guiard, B., Voos, W., Li, Y., Lind, M., Meisinger, C., Geissler, A., Sickmann, A., Meyer, H. E., Bilanchone, V., Cumsky, M. G., Truscott, K. N., Pfanner, N., and Rehling, P. (2004) *Nat. Struct. Mol. Biol.* **11,** 226–233
16. Westermann, B., Prip-Buus, C., Neupert, W., and Schwarz, E. (1995) *EMBO J.* **14,** 3452–3460
17. Laloraya, S., Gambill, B. D., and Craig, E. A. (1994) *Proc. Natl. Acad. Sci. U. S. A.* **91,** 6481–6485
18. Bolliger, L., Deloche, O., Glick, B. S., Georgopoulos, C., Jeno, P., Kronidou, N., Horst, M., Morishima, N., and Schatz, G. (1994) *EMBO J.* **13,** 1998–2006

[4] D. Mokranjac, unpublished data.

19. Chacinska, A., Lind, M., Frazier, A. E., Dudek, J., Meisinger, C., Geissler, A., Sickmann, A., Meyer, H. E., Truscott, K. N., Guiard, B., Pfanner, N., and Rehling, P. (2005) *Cell* **120,** 817–829
20. Popov-Celeketic, D. S., Mapa, K., Neupert, W., and Mokranjac, D. (2008) *EMBO J.* **27,** 1469–1480
21. Geissler, A., Chacinska, A., Truscott, K. N., Wiedemann, N., Brandner, K., Sickmann, A., Meyer, H. E., Meisinger, C., Pfanner, N., and Rehling, P. (2002) *Cell* **111,** 507–518
22. Yamamoto, H., Esaki, M., Kanamori, T., Tamura, Y., Nishikawa, S., and Endo, T. (2002) *Cell* **111,** 519–528
23. Mokranjac, D., Paschen, S. A., Kozany, C., Prokisch, H., Hoppins, S. C., Nargang, F. E., Neupert, W., and Hell, K. (2003) *EMBO J.* **22,** 816–825
24. Alder, N. N., Sutherland, J., Buhring, A. I., Jensen, R. E., and Johnson, A. E. (2008) *Mol. Biol. Cell* **19,** 159–170
25. Davis, G. D., Elisee, C., Newham, D. M., and Harrison, R. G. (1999) *Biotechnol. Bioeng.* **65,** 382–388
26. Sikorski, R. S., and Hieter, P. (1989) *Genetics* **122,** 19–27
27. Vernet, T., Dignard, D., and Thomas, D. Y. (1987) *Gene* (*Amst.*) **52,** 225–233
28. Donzeau, M., Kaldi, K., Adam, A., Paschen, S., Wanner, G., Guiard, B., Bauer, M. F., Neupert, W., and Brunner, M. (2000) *Cell* **101,** 401–412
29. Bauer, M. F., Sirrenberg, C., Neupert, W., and Brunner, M. (1996) *Cell* **87,** 33–41
30. Meinecke, M., Wagner, R., Kovermann, P., Guiard, B., Mick, D. U., Hutu, D. P., Voos, W., Truscott, K. N., Chacinska, A., Pfanner, N., and Rehling, P. (2006) *Science* **312,** 1523–1526
31. Dyson, H. J., and Wright, P. E. (2005) *Nat. Rev. Mol. Cell. Biol.* **6,** 197–208